Ouyang *et al. Cancer Cell International* (2025) 25:172
https://doi.org/10.1186/s12935-025-03789-9

Cancer Cell International

RESEARCH

Open Access

# Genomic signatures in plasma circulating tumor DNA reveal treatment response and prognostic insights in mantel cell lymphoma

Zhou Ouyang[1†], Ruolan Zeng[1†], Song Wang[2], Xiaoying Wu[2], Yajun Li[1], Yizi He[1], Caiqin Wang[1], Chen Xia[1], Qiuxiang Ou[2], Hua Bao[2], Wei Yang[2], Ling Xiao[3*] and Hui Zhou[1*]

## Abstract

**Background** Mantle cell lymphoma (MCL) is an aggressive subtype of B-cell non-Hodgkin's lymphoma. The applicability of circulating tumor DNA (ctDNA) for predicting treatment response and prognosis in MCL remains underexplored.

**Methods** This study included 34 MCL patients receiving first-line chemoimmunotherapy. We assessed the ability of plasma ctDNA to detect tumor-specific genetic alterations and explored its potential as a noninvasive biomarker for treatment response and prognosis in MCL.

**Results** Commonly mutated genes in MCL included *CCND1* (93.5%), *ATM* (48.4%), *KMT2D* (25.8%), and *TP53* (25.8%). Subgroup analysis of tissue samples showed that *CDKN2A* mutations ($P=0.028$), along with alterations in BCR and TCR signaling ($P=0.004$) and the PI3K pathway ($P=0.008$), were enriched in the blastoid subtype. *ATM* mutations ($P=0.041$) were more prevalent in MIPI-low patients, while epigenetic chromatin remodeling pathway alterations ($P=0.028$) were more common in MIPI-high patients. Plasma ctDNA demonstrated high sensitivity for detecting structural variants (96.6%), followed by mutations (71.3%) and copy number variants (30.0%). 75% of patients exhibited moderate-to-high concordance in detecting genomic variants between plasma and tissue samples. Pretreatment ctDNA levels exhibited high specificity in predicting clinical efficacy but had a suboptimal sensitivity of 68.2%. Higher ctDNA levels were significantly associated with shorter progression-free survival (PFS; $P=0.002$) and overall survival (OS; $P=0.009$). Additional ctDNA-based genetic features associated with shorter PFS included *TP53* ($P=0.002$), *TRAF2* ($P=0.023$), and *SMARCA4* ($P=0.023$) mutations, while *TP53* ($P=0.006$) and *TERT* ($P=0.031$) mutations predicted shorter OS. Persistent positive ctDNA in post-treatment plasma samples indicated molecular relapse and poor prognosis, whereas undetectable ctDNA defined a subset of patients with favorable survival outcomes.

[†]Zhou Ouyang and Ruolan Zeng have contributed equally to this work.

*Correspondence:
Ling Xiao
xiaolingcsu@csu.edu.cn
Hui Zhou
zhouhui9403@126.com
Full list of author information is available at the end of the article

**Conclusions** This study identified plasma ctDNA as a promising biomarker that noninvasively captures tumor-derived genetic variants associated with treatment response and survival outcomes in MCL, highlighting the clinical value of ctDNA for diagnosis, recurrence prediction, and surveillance monitoring.

**Keywords** Mantle cell lymphoma, Circulating tumor DNA, Chemoimmunotherapy, Biomarker

## Background

Mantle cell lymphoma (MCL) is a rare but aggressive subtype of B-cell non-Hodgkin's lymphoma. According to the World Health Organization (WHO) classification of lymphoid neoplasms [1], MCL is primarily categorized into two types based on biological behaviors: conventional MCL, accounting for 80–90% of cases, which typically has an aggressive clinical course and is characterized by unmutated immunoglobulin heavy chain variable region (IGHV) genes and expression of sex-determining regions-Y box transcription factor 11 (SOX-11); and leukemic nonnodal MCL, representing 10–20% of cases, which generally shows an indolent biological behavior with negative SOX-11 expression and somatic hypermutation of IGHV. Conventional MCL includes more aggressive blastoid and pleomorphic subtypes upon acquiring additional molecular alterations [2, 3].

Advances in understanding molecular pathogenesis, prognosis, and treatments have led to significant progress in the management of MCL. For symptomatic fit patients, rituximab-based chemotherapies with or without autologous stem cell transplantation (ASCT) remain the standard first-line treatment [3]. Additional options for relapsed or refractory diseases include Bruton's tyrosine kinase (BTK) inhibitors [4–6], Bcl-2 antagonists [7], and anti-CD19-chimeric antigen receptor therapy (CAR-T) [8]. Despite these advancements, drug resistance and frequent relapses remain challenging in MCL. Key clinical factors, such as age, advanced stage, elevated lactate dehydrogenase (LDH) and β2-microglobulin levels, blastoid morphology, and extranodal disease, have been associated with worse clinical outcomes [3]. Additional prognostic markers already in clinical use or showing potential for future application include the MCL International Prognostic Index (MIPI) [9], Ki-67 expression, TP53 expression [10], and specific genetic lesions [11–13], such as *TP53* mutations, *CKDN2A* deletions, and mutations in *NOTCH* genes, *KMT2D*, *MYC*, *WHSC1*, and *CCND1*. Improved knowledge of MCL's molecular biology and identification of prognostic factors could further support personalized therapeutic strategies to improve survival outcomes.

Response assessment in lymphoma primarily relies on computed tomography (CT) and $^{18}$fluoro-2-deoxyglucose positron emission tomography (PET) scans. However, since disease recurrence often originates from residual tumors below the threshold of clinical detection, imaging scans alone may lack the sensitivity to predict clinical relapse. While pathological examination of tissue specimens remains the diagnostic gold standard, invasive tissue biopsies are inadequate for capturing the temporal heterogeneity of tumors, especially as lymphomas can evolve under therapeutic pressure. In this context, liquid biopsies, which gather genetic information from all disease sites, show great potential as noninvasive biomarkers in both hematologic and solid tumors, addressing key limitations of traditional clinical tools. The tumor-derived fraction of cell-free DNA, known as circulating tumor DNA (ctDNA), is the most extensively studied form of liquid biopsy and has been investigated for monitoring treatment response and detecting relapse in aggressive lymphomas, such as diffuse large B-cell lymphoma and Hodgkin lymphoma [14–21]. However, continued research is needed to extend these clinical applications, including diagnostic and surveillance monitoring for early relapse detection, to other non-Hodgkin lymphomas, such as MCL.

In this study, we analyzed baseline tissue and plasma samples from 34 MCL patients treated with first-line chemotherapy. We compared somatic genetic variants identified across different sample types, focusing on actionable genetic alterations and recurrent mutations in MCL. Additionally, we assessed the clinical utility of pretreatment ctDNA for predicting treatment response and survival outcomes. Furthermore, dynamic changes in longitudinal plasma ctDNA demonstrated the potential to reflect tumor burden and inform disease progression, thus guiding timely response-adapted strategies.

## Materials and methods

### Patients and sample collection

This retrospective study enrolled 34 patients diagnosed with MCL and treated at the participating hospital between January 2020 and December 2022. The primary inclusion criteria were as follows: (1) pathological confirmation of conventional MCL based on the 2016 WHO classification of lymphomas [1]; (2) presence of at least one measurable lesion (nodal lesions with a diameter > 1.5 cm, and extranodal lesions with a diameter > 1 cm, both FDG-PET positive); (3) availability of pretreatment tissue biopsy and/or plasma sample for genomic profiling; and (4) completion of at least one cycle of systemic

treatment with an accompanying treatment response evaluation. The exclusion criteria were: (1) presence of severe inflammatory diseases or complications; (2) receipt of prior anti-tumor therapy before initiating chemotherapy; (3) diagnosis of recurrent disease; and (4) expected life expectancy < 3 months. All patients received standard first-line treatment regimens. Clinical data for each patient were obtained from medical records. Staging was classified according to the Ann Arbor staging system, while treatment response was evaluated using the Lugano response criteria for non-Hodgkin lymphoma [22]. Lymph node biopsies and bone marrow aspirations were obtained at baseline, while serial peripheral blood samples were collected at baseline, midterm induction (after four cycles), end of induction, and follow-up visits. All study procedures were approved by the institutional review board (Ethics Approval Number: No.2024-152) and conducted in accordance with the principles of the Helsinki Declaration. All patients provided written informed consent for participation and publication.

### Sample processing, library construction, and next-generation sequencing

Genomic DNA from bone marrow or formalin-fixed paraffin-embedded samples from lymph nodes was extracted using the Qiagen DNeasy Blood & Tissue Kit (QIAGEN, Dusseldorf, Germany). The plasma fraction of the peripheral blood was isolated within two hours after specimen collection, which was first centrifuged at 1800×*g* for 10 min, followed by cfDNA extraction and purification using the QIAamp Circulating Nucleic Acid Kit (QIAGEN, Dusseldorf, Germany). Genomic DNA from oral swabs was prepared using the Qiagen DNeasy Blood & Tissue Kit (QIAGEN, Dusseldorf, Germany) as the normal control for filtering germline mutations. Genomic DNA was quantified using the dsDNA HS assay kit on a Qubit 3.0 fluorometer (Life Technology, US), followed by NGS library construction using the KAPA Hyper Prep kit (KAPA Biosystems). Hyrbidization-based target enrichment was performed using a customized xGen lockdown probes panel covering 475 hematopoietic and lymphoid neoplasm-related genes (Hermasalus™, Nanjing Geneseeq Technology Inc., Nanjing, China) (Supplementary Table S1). Library fragment size was analyzed on a Bioanalyzer 2100 using the High Sensitivity DNA Kit (Agilent Technologies, Santa Clara, CA). Prepared libraries were sequenced on the Illumina HiSeq4000 platform (Illumina, San Diego, USA).

### NGS data processing and mutation calling

Trimmomatic [23] was used for FASTQ file quality control, with reads below 15 and those containing N bases removed. Sequencing reads were aligned to the reference human genome hg19 using the Burrows-Wheeler Aligner (BWA, https://github.com/lh3/bwa/tree/master/bwakit). PCR duplicates were removed with Picard (https://broadinstitute.github.io/picard/). Local alignment and base quality score recalibrations were performed using GATK3 (https://software.broadinstitute.org/gatk/). Somatic single nucleotide variants (SNV) and insertion/deletions (indels) were called using VarScan2 [24], and subsequently annotated with ANNOVAR against multiple databases, including dbSNP (v138), 1000Genome, ExAC, COSMIC (v70), ClinVAR, and SIFT [25]. Copy number variation (CNV) analysis was conducted using FACETS [26]. Detection of structural variants (SV) was carried out using icallSV [27] and annotated with iAnnotateSV [28]. Variants were filtered based on the following criteria: (i) absence in matched genomic DNA from normal control; and (ii) frequency ≤ 1% in the 1000 Genomes Project or the Exome Aggregation Consortium's 65,000 exomes database. To qualify as true variants, SNVs/indels and SVs required a variant allele frequency (VAF) ≥ 0.5% with ≥ 3 supporting reads for lymph node samples, or VAF ≥ 0.1% with ≥ 3 supporting reads for plasma and bone marrow samples. CNVs were classified as gains or losses based on gene ratios: ≥ 2.0 for gains and < 0.6 for losses in lymph node samples [29], and ≥ 1.6 for gains and < 0.6 for losses in plasma and bone marrow samples [30]. All variants were manually reviewed using the Integrative Genomics Viewer, and the final curated list was refined to focus on somatic alterations within canonical signaling pathways representing key cancer hallmarks [31], as well as pathways frequently altered in MCL (Supplementary Table S2).

### Measurement of ctDNA levels

The ctDNA level for each sample was quantified as haploid genome equivalents (hGE) per milliliter of plasma (hGE/mL) using the formula: [(the mean VAF for all mutations detected) x cfDNA concentration (pg/mL of plasma)] ÷3.3, as previously described [16]. The base-10 logarithmic transformed value was applied for analysis.

### Statistical analysis

All statistical analyses were performed in R (version 4.1.3). Categorical variables were compared between groups using Fisher's exact test. Non-paired comparisons of continuous variables were performed using the Wilcoxon rank-sum test or Kruskal Wallis test, as appropriate. Linear correlations were evaluated using Spearman's test. The Jonckheere-Terpstra test was used to detect a trend between a non-normally distributed dependent variable and an ordered independent variable, while the Cochran-Armitage trend test was used to evaluate the presence of a trend between a binary

dependent variable and an independent variable with more than two ordered categories. Cohen's Kappa coefficients (κ) were calculated to present the concordance of somatic variant detection between plasma and tissue samples. Progression-free survival (PFS) was defined as the time from first-line treatment initiation to tumor progression or death, whichever occurs first. Overall survival (OS) was calculated from the date of diagnosis to the date of death from any cause. Event-time distributions were estimated using Kaplan–Meier methodology, with statistical differences assessed using the log-rank test. Cox proportional hazard models were fitted to estimate hazard ratios (HR) with 95% confidence intervals (CI), and the proportionality of hazards was assessed using log(-log) survival plots. Kyoto Encyclopedia of Genes and Genomes (KEGG) analysis was performed using the R package "ClusterProfiler". A two-sided *P*-value of less than 0.05 was considered significant for all tests unless otherwise indicated (*$P < 0.05$, **$P < 0.01$, ***$P < 0.001$).

## Results

### Patient characteristics

This study included thirty-four MCL patients who received first-line therapy followed by response evaluation (Table 1). The median age of patients was 59 years (interquartile range [IQR]: 52–67 years), with 73.5% (25/34) of patients being under the age of 65. Most patients were diagnosed with stage IV disease (94.1%, 32/34), and 79.4% (27/34) had the classic subtype of MCL, compared to 20.6% (7/34) presented with the more aggressive blastoid subtype. B symptoms, characterized by unexplained weight loss, night sweats, or fever, were rarely reported. The MIPI score, which incorporates age, performance status, LDH levels, and leukocyte count, was utilized to assess individual risk profiles at baseline. Of all these patients, 61.8% (21/34) were classified as low-risk, while 5 (14.7%) and 8 (23.5%) patients were categorized as high- and intermediate-risk, respectively. Extranodal infiltration was observed in 32 patients, with the bone marrow being the most frequently affected site, followed by the intestines (Supplementary Fig. S1). Following first-line therapy, 85.3% (29/34) of patients underwent ASCT, and 67.6% (23/34) received maintenance therapy. Patients were categorized into complete response (CR; N = 24) and non-CR (N = 10) groups based on their best response to first-line treatment. Non-CR patients were more likely to have higher MIPI scores ($P = 0.002$), the combined MIPI scores (MIPI-c; $P = 0.004$), serum LDH levels ($P = 0.037$), and β2-microglobulin levels ($P = 0.016$). No significant differences in other clinical features were found between the two subgroups.

### Genomic characterization of MCL using tissue samples

Treatment-naïve tissue biopsies were available for 31 patients and analyzed through genomic profiling using an NGS panel that targets 475 genes related to hematopoiesis and lymphoid neoplasms (Fig. 1). The most commonly mutated genes were *CCND1* (93.5%), followed by *ATM* (48.4%), *KMT2D* (25.8%), *TP53* (25.8%), *CDKN2A* (12.9%), *NFKBIE* (12.9%), *NSD2* (12.9%), and *TRAF2* (12.9%) (Fig. 2A). At the pathway level, 93.5% (29/31) of patients harbor cell cycle pathway genomic aberrations, and 67.7% (21/31) with an altered TP53 signaling pathway. Subgroup analysis further revealed that the prevalence of *CDKN2A* alterations was significantly higher in the blastoid subtype of MCL compared to the classic subtype (42.9% vs. 4.2%, $P = 0.028$) (Fig. 2B). Additionally, genetic alterations related to the B cell antigen receptor (BCR) and endosomal Toll-like receptor (TCR) signaling (85.7% vs. 20.8%, $P = 0.004$) as well as the PI3K pathway (42.9% vs. 0%, $P = 0.008$) were also significantly enriched in the aggressive subtype. Interestingly, *ATM* mutations were more commonly identified in patients with low scores on MIPI (57.9% vs. 0%, $P = 0.041$), whereas epigenetic chromatin remodeling pathway alterations were more frequent in MIPI-high patients (80% vs. 21.1%, $P = 0.028$) (Fig. 2C). Although there was a trend in higher mutational frequencies of mutations in *TP53*, *KMT2D*, and *TRAF2* in high-risk patients stratified by MIPI scores, no statistical significance was achieved.

We then compared the mutational landscape of patients based on treatment response and found that genes, including *CCND1*, *ATM*, *KMT2D*, *TP53*, and *CDKN2A*, remained the most frequently mutated in both CR and non-CR groups (Supplementary Fig. S2 A). *TP53* mutations (50% vs. 14.3%, $P = 0.074$) and *TRAF2* mutations (30% vs. 4.8%, $P = 0.087$) were more prevalent in non-CR patients compared to CR patients, but the differences were not statistically significant (Supplementary Fig. S2B). KEGG pathway analysis revealed similar functional enrichment of gene mutations between subgroups, with cancer-associated pathways prominently featured among the top enriched functions (Supplementary Fig. S2 C). However, while *CARD11* and *NFKBIE* mutations were concurrently identified in both CR and non-CR patients relating to T cell and B cell receptor signaling, differences may exist between subgroups in a range of pathways associated with antitumor immunity, potentially reflecting distinct immunological characteristics (Supplementary Fig. S2D). Notably, *TP53* mutations, *TRAF2* mutations, and alterations in the epigenetic chromatin remodeling pathway were associated with shorter progression-free survival (PFS) ($P = 0.005$, $P = 0.007$, and $P = 0.063$, respectively), with a consistent trend toward poorer overall survival (OS) ($P = 0.124$, $P = 0.054$, and

**Table 1** Clinical characteristics of patients

| | All (N = 34) | CR (N = 24) | Non-CR (N = 10) | *P*-value |
|---|---|---|---|---|
| Age | | | | 0.085 |
| ≤ 65 years | 25 (73.5%) | 20 (83.3%) | 5 (50.0%) | |
| > 65 years | 9 (26.5%) | 4 (16.7%) | 5 (50.0%) | |
| Median (IQR) | 59 (52–67) | 56 (52–61) | 66 (57–69) | |
| Sex | | | | > 0.999 |
| Female | 10 (29.4%) | 7 (29.2%) | 3 (30.0%) | |
| Male | 24 (70.6%) | 17 (70.8%) | 7 (70.0%) | |
| Ann Arbor stage | | | | > 0.999 |
| II | 1 (2.9%) | 1 (4.2%) | 0 (0%) | |
| III | 1 (2.9%) | 1 (4.2%) | 0 (0%) | |
| IV | 32 (94.1%) | 22 (91.7%) | 10 (100%) | |
| Histologic subtype | | | | 0.157 |
| Classic | 27 (79.4%) | 21 (87.5%) | 6 (60.0%) | |
| Blastoid | 7 (20.6%) | 3 (12.5%) | 4 (40.0%) | |
| B symptoms | | | | 0.067 |
| Yes | 4 (11.8%) | 1 (4.2%) | 3 (30.0%) | |
| No | 30 (88.2%) | 23 (95.8%) | 7 (70.0%) | |
| Ki-67 expression | | | | 0.437 |
| < 30% | 11 (32.4%) | 9 (37.5%) | 2 (20.0%) | |
| ≥ 30% | 23 (67.6%) | 15 (62.5%) | 8 (80.0%) | |
| MIPI | | | | 0.002** |
| Low | 21 (61.8%) | 19 (79.2%) | 2 (20.0%) | |
| Intermediate | 8 (23.5%) | 4 (16.7%) | 4 (40.0%) | |
| High | 5 (14.7%) | 1 (4.2%) | 4 (40.0%) | |
| MIPI-c | | | | 0.004** |
| Low | 9 (26.5%) | 8 (33.3%) | 1 (10.0%) | |
| Low-moderate | 13 (38.2%) | 12 (50.0%) | 1 (10.0%) | |
| Moderate-high | 8 (23.5%) | 3 (12.5%) | 5 (50.0%) | |
| High | 4 (11.8%) | 1 (4.2%) | 3 (30.0%) | |
| Extranodal involvement | | | | > 0.999 |
| Yes | 32 (94.1%) | 2 (8.3%) | 0 (0%) | |
| No | 2 (5.9%) | 22 (91.7% | 10 (100%) | |
| Chemotherapy regimen | | | | 0.077 |
| R-CHOP | 10 (29.4%) | 4 (16.7%) | 6 (60.0%) | |
| R-CHOP/DHAP | 17 (50.0%) | 13 (54.2%) | 4 (40.0%) | |
| R-CHOP/BAC | 1 (2.9%) | 1 (4.2%) | 0 (0%) | |
| R-DA-EPOCH/DHAP | 1 (2.9%) | 1 (4.2%) | 0 (0%) | |
| BR | 5 (14.7%) | 5 (20.8%) | 0 (0%) | |
| Best overall response | | | | ~ |
| CR | 24 (70.6%) | 24 (100%) | 0 (0%) | |
| PR | 5 (14.7%) | 0 (0%) | 5 (50.0%) | |
| SD | 2 (5.9%) | 0 (0%) | 2 (20.0%) | |
| PD | 3 (8.8%) | 0 (0%) | 3 (30.0%) | |
| ASCT | | | | 0.291 |
| Yes | 5 (14.7%) | 5 (20.8%) | 0 (0%) | |
| No | 29 (85.3%) | 19 (79.2%) | 10 (100%) | |
| Maintenance therapy | | | | 0.005** |
| Yes | 23 (67.6%) | 20 (83.3%) | 3 (30.0%) | |
| No | 11 (32.4%) | 4 (16.7%) | 7 (70.0%) | |

**Table 1** (continued)

| | All (N = 34) | CR (N = 24) | Non-CR (N = 10) | *P*-value |
|---|---|---|---|---|
| LDH (U/L) | | | | 0.037* |
| Median (IQR) | 191.1 (160.6–231.3) | 177.5 (158.7–213.0) | 229.5 (194.3–325.5) | |
| β2-microglobulin (mg/L)[a] | | | | 0.016* |
| Median (IQR) | 3.24 (2.53–4.29) | 3.03 (2.30–3.61) | 4.46 (3.36–5.78) | |

Statistical significance is denoted by asterisks: *$P < 0.05$ and **$P < 0.01$

*IQR* interquartile range, *CR* complete response, *PR* partial response, *SD* stable disease, *PD* progressive disease, *MIPI* MCL international prognostic index, *ASCT* autologous stem cell transplantation, *LDH* lactate dehydrogenase, *R* Rituximab, *CHOP* cyclophosphamide/doxorubicin/vincristine/prednisone, *DHAP* dexamethasone/high-dose cytarabine/cisplatin, *BAC* bendamustine/cytarabine, *EPOCH* etoposide/prednisone/vincristine/cyclophosphamide/doxorubicin, *BR* rituximab/bendamustine

[a] Data was available for 32 patients, including 23 CR and 9 non-CR patients

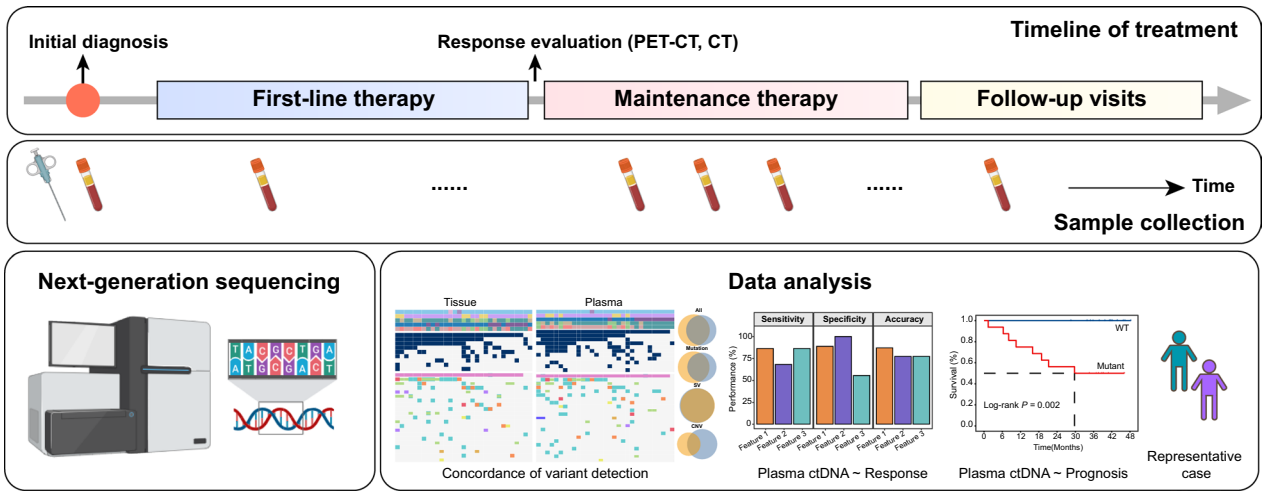


**Fig. 1** Overview of study design. Baseline tissue biopsies and plasma ctDNA from 34 MCL patients receiving first-line chemotherapy were analyzed using targeted next-generation sequencing to characterize the mutational landscape and assess the concordance of somatic genomic variant detection between paired samples. Pretreatment ctDNA was further investigated to evaluate its association with treatment response and prognosis. Longitudinal plasma samples from representative patients highlighted the importance of interim ctDNA monitoring for disease surveillance

(See figure on next page.)

**Fig. 2** Genomic profiling using baseline tissue samples. **A** Mutational landscape of patients using treatment-naive tissue samples. The genomic profiles focused on individual genes with a mutation count ≥ 2, actionable genes annotated by OncoKB, and signaling pathways with a mutation count ≥ 3. **B**, **C** Bar plots showing the prevalence of gene alterations and pathways stratified by histological subtype (**B**) or the MCL International Prognostic Index (MIPI) (**C**). **D**, **E** Kaplan–Meier survival curves showing the associations between genetic alterations/pathways and progression-free survival (**D**) and overall survival (**E**). **F** Lollipop plot highlighting the specific *ATM* mutation sites identified in baseline tissue samples. **G** Multivariate Cox regression analysis for progression-free survival incorporating significant clinical and mutational features identified in the univariate analysis

$P = 0.031$, respectively) (Fig. 2D, E). In contrast, *ATM* mutations were significantly associated with prolonged PFS ($P = 0.007$) and OS ($P = 0.009$), highlighting their potential as a favorable prognostic biomarker in MCL. The ataxia telangiectasia mutated (*ATM*) gene plays a crucial role in regulating cell cycle progression and DNA damage repair. Of the 22 *ATM* mutations, 9 (40.9%) were truncating mutations, 11 (50%) were missense mutations, and the remaining two were inframe mutations (Fig. 2F). Multivariate analysis incorporating relevant clinical features identified MIPI and *TP53* mutations as significant risk factors for shorter PFS, while maintenance treatment and *ATM* mutations were associated with longer PFS (Fig. 2G; Supplementary Table S3).

### ctDNA noninvasively captures tumor-specific genetic aberrations

Given the inherent limitations of tissue biopsies, plasma-derived ctDNA, which gathers genetic information from all disease sites, holds significant promise as a

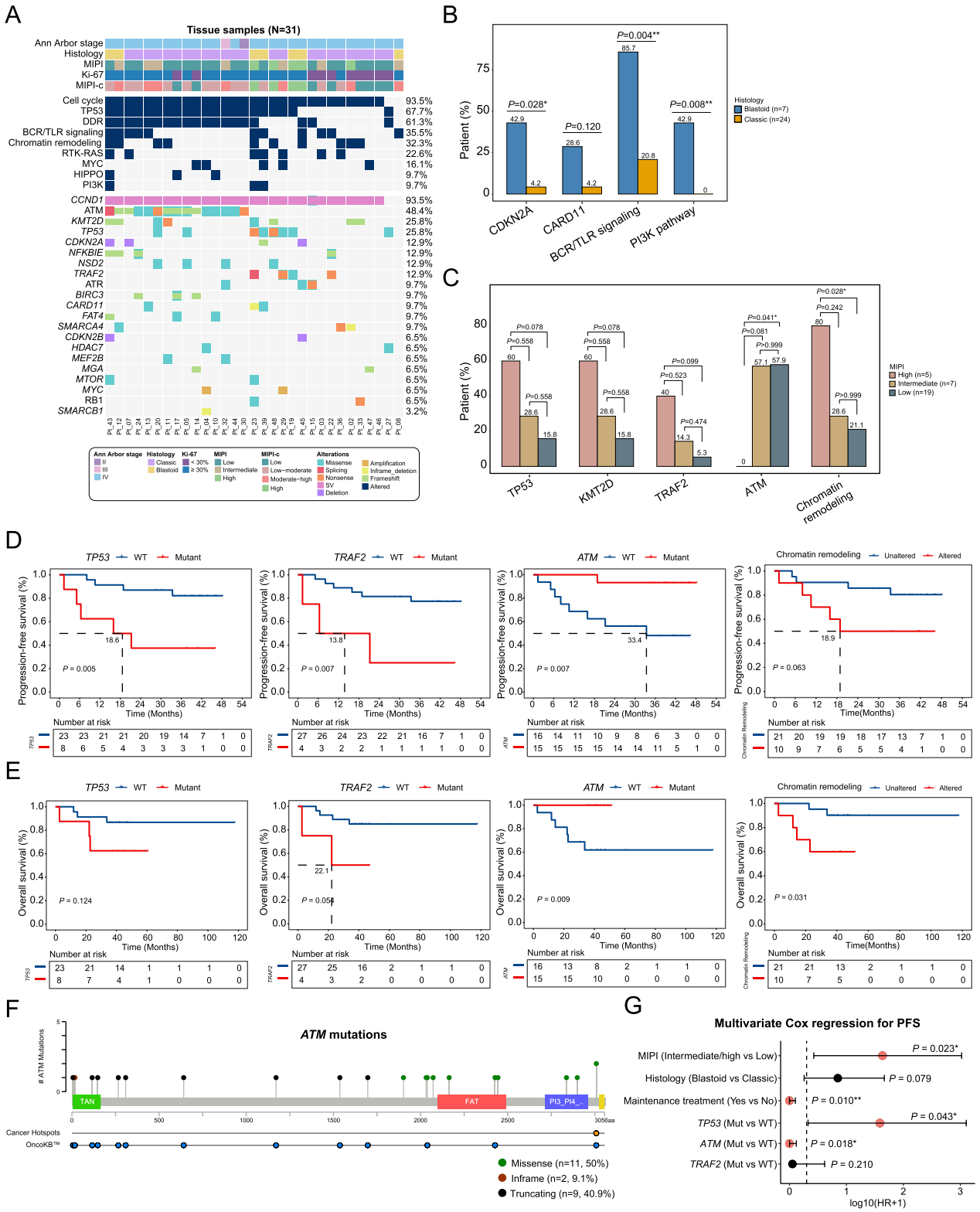


**Fig. 2** (See legend on previous page.)

noninvasive biomarker for both hematologic and solid tumors. Consistently, *CCND1* fusions and mutations in *ATM*, *KMT2D*, and *TP53* were identified as the top four genetic variants in plasma samples (Fig. 3A). Additional genes with a high mutation frequency in both tissue and plasma samples included *NSD2* and *TRAF2*.

Comparing the genomic profiles of patients with paired samples (N = 28), 66.3% (118/178) of tissue-based somatic variants were detected in paired plasma samples with a detection sensitivity of 73.3% (Fig. 3B, C). Sixty genetic variants were exclusively identified in plasma but not tissue samples, underscoring the potential of plasma ctDNA in identifying relevant mutations missed by the original tissue biopsy. For each variant type, ctDNA demonstrated the highest detection sensitivity for SVs (96.6%), followed by SNVs/indels (71.3%) and CNV (30%) (Fig. 3C). Remarkably, all tissue-based SVs were detected in paired plasma samples, in which one additional SV was observed. At the patient level, the median kappa (κ) coefficient was 0.71 (IQR: 0.62–0.88), with 75% of patients (21/28) exhibiting a κ ≥ 0.6, indicating at least a "moderate" level of agreement in detecting all 475 genes covered by the targeted panel between paired samples (Fig. 3D). The only exception was patient 33 (Pt_33), who displayed a poor statistical consistency in variant detection between paired samples. This discrepancy could be attributed to the extreme imbalance in data, given that only one single *DNMT3A* splicing variant was identified

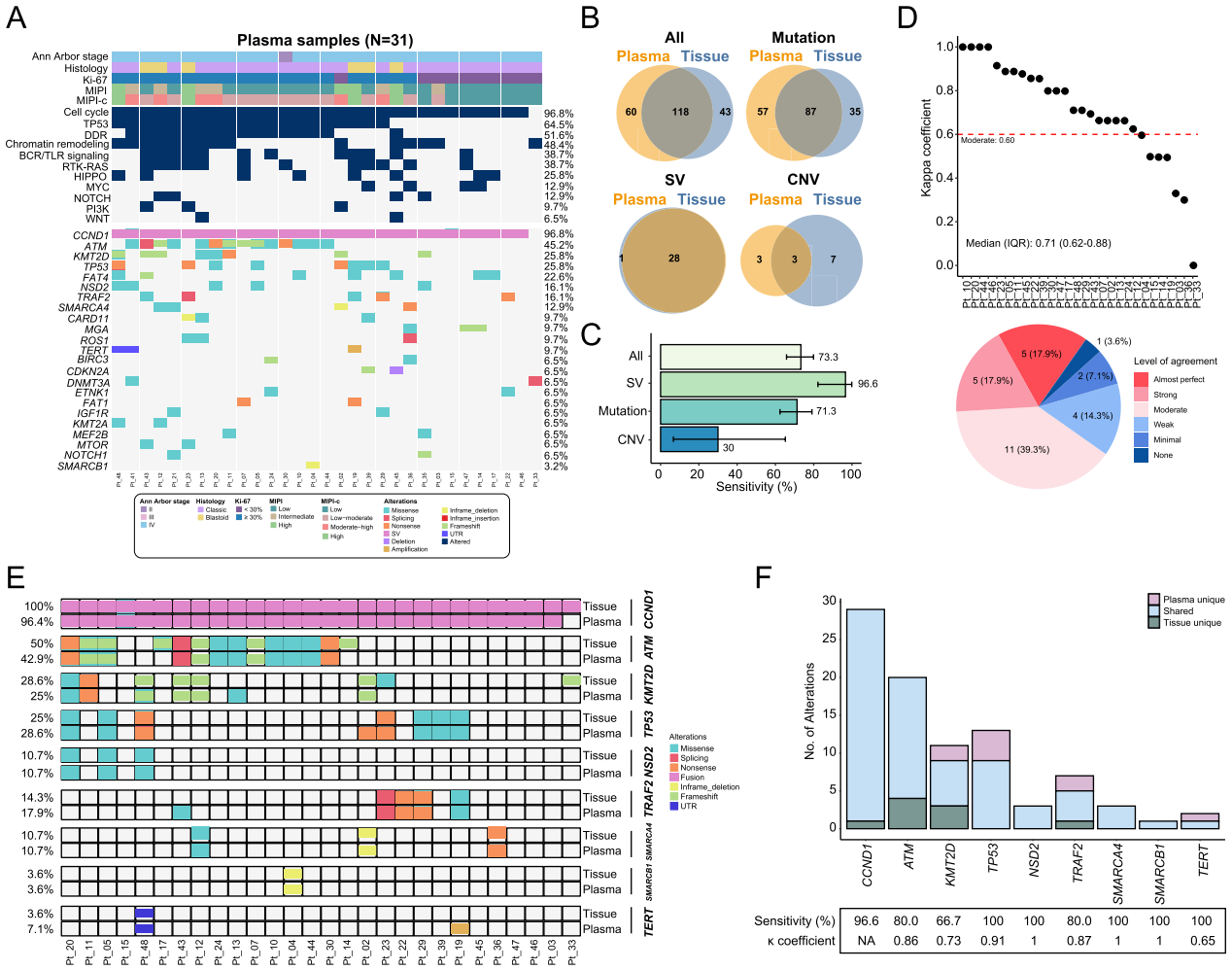


**Fig. 3** Concordance of genomic variant detection between paired samples. **A** Mutational landscape of patients using pretreatment plasma samples. The genomic profiles focused on individual genes and pathways with a mutation count ≥ 2, as well as actionable genes annotated by OncoKB. **B** Venn diagrams depicting the number of shared and unique variants detected in paired samples for each variant type. **C** Bar plots illustrating the detection sensitivity of plasma ctDNA for all variants and each variant subtype. **D** Patient-level agreement for variant detection between paired samples, considering all genes covered by the targeted panel. **E** Heatmap showing the detection of genes with high mutational frequency and those with clinical actionability. **F** Stacked bar plot showing the number of shared and unique mutations for genes of interest

in the plasma sample. Using tissue samples as the gold standard, ctDNA demonstrated high sensitivity in detecting recurrent mutations and clinically actionable genes annotated by OncoKB [32], with sensitivity ranging from 66.7% to 100% (Fig. 3E, F). Furthermore, the concordance between paired samples was generally satisfactory, with the lowest κ of 0.65 for detecting telomerase reverse transcriptase (*TERT*) mutations.

Although lymph node biopsies remain the gold standard for diagnosis, bone marrow (BM) aspiration is a routine part of staging and should be considered when assessing variant detection, especially in clinical scenarios where lymph node biopsy is not feasible or when the disease primarily involves the BM. Here, we analyzed the mutational profiles of 17 patients with available samples from lymph nodes, BM, and plasma, and compared variant detection performance across these three sample types. Consistently, the most commonly mutated genes identified in BM were *CCND1*, *ATM*, *TP53*, and *KMT2D* (Supplementary Fig. S3 A). However, BM samples failed to detect two *CCND1* fusions that were concurrently identified in both tissue and plasma samples. Furthermore, BM samples demonstrated limited detection ability for CNVs, even though their overall sensitivity for mutations (94.3%) and SV (88.2%) were comparable to plasma samples, especially for actionable targets and recurrent mutations in MCL (Supplementary Fig. S3B–E).

#### Correlates of plasma ctDNA to treatment response in MCL

We then investigated the correlation between plasma ctDNA and treatment response. The median plasma ctDNA level was 176.2 hGE/mL (IQR: 64.4–1094.7 hGE/mL) (Supplementary Fig. S4 A). Elevated ctDNA levels were significantly associated with various clinical features, including the blastoid subtype ($P = 0.053$), BM infiltration ($P = 0.014$), higher MIPI scores ($P = 0.002$), increased extranodal involvement ($P = 0.025$), and higher levels of LDH ($P < 0.001$), Ki-67 ($P < 0.001$), and β2-microglobulin ($P < 0.001$) in MCL (Supplementary Fig. S4B–H). Importantly, plasma ctDNA levels were significantly associated with therapeutic response, with CR patients showing significantly lower ctDNA levels than non-CR patients ($P = 0.001$) (Fig. 4A, B). Additionally, *TP53* mutations and alterations in the BCR/TLR signaling pathway were more frequently observed in non-CR patients ($P = 0.027$ and $P = 0.056$, respectively), suggesting a negative association with treatment response and potentially worse survival in MCL patients (Fig. 4C, D). Compared to the prognostic index MIPI, ctDNA levels, using the median as the cutoff, exhibited 100% specificity in distinguishing non-CR from CR patients, while *TP53* mutational status demonstrated comparable sensitivity in predicting treatment response (Fig. 4E, F). All patients with low ctDNA levels and no detectable *TP53* variants achieved CR, while those with high ctDNA levels and *TP53* mutations showed a significantly lower CR rate (Cochran Armitage test, $P = 0.001$) (Fig. 4G). Testing alternative cutoffs for ctDNA levels yielded consistent results (Supplementary Fig. S4I–K). However, in smaller cohorts, the median cutoff may be more susceptible to variability due to cohort composition and patient-specific factors, such as demographics and clinical characteristics, which should be considered when determining an optimal threshold.

#### Prognostic value of pretreatment ctDNA in MCL

Next, we assessed whether baseline ctDNA levels and genomic features identified in plasma ctDNA could inform the survival outcomes of MCL patients. Cox regression analysis identified 7 plasma ctDNA-based features significantly associated with PFS, including ctDNA levels ($P = 0.002$), *TP53* mutations ($P = 0.002$), *TRAF2* mutations ($P = 0.023$), *SMARCA4* mutations ($P = 0.023$), and alterations in the BCR/TLR ($P = 0.015$), PI3K ($P = 0.019$), and NOTCH ($P = 0.019$) pathways (Fig. 5A; C–G; Supplementary Fig. S5 A, B). Among these, ctDNA levels ($P = 0.009$), *TP53* mutations ($P = 0.006$), and altered BCR/TLR ($P = 0.010$) and PI3K ($P = 0.002$) pathways were significant risk factors for poorer overall survival, with a consistent trend observed for *TRAF2* mutations (Fig. 5B; H–L). Additionally, *TERT* mutations were significantly correlated with shorter OS ($P = 0.031$), with a similar trend observed for PFS (Supplementary Fig. S5 C). *TP53* mutations and *TRAF2* mutations were also identified as unfavorable biomarkers for PFS in tissue profiling (Fig. 2D). Consistent trends between tissue and plasma profiling were observed for *ATM* mutations and alterations in the epigenetic chromatin remodeling pathway, although these did not reach statistical significance, given that only 28 patients having paired samples (Supplementary Fig. S5D, E).

To validate these prognostic associations, we analyzed an external dataset of 158 MCL patients with OS data [33]. Consistently, patients with *TP53* mutations had significantly shorter OS compared to those with wild-type tumors (median OS: 23.6 vs. 64.7 months, $P < 0.001$) (Supplementary Fig. S5 F). Similarly, *SMARCA4* mutations correlated with poorer OS (median OS: 28.7 vs. 63.1 months, $P = 0.012$). Alterations in the BCR/TLR pathway and epigenetic chromatin remodeling pathway were also linked to shorter OS. However, *ATM* mutations did not show a significant association with prognosis in this dataset ($P = 0.43$). The frequency of *ATM* mutations in the external dataset was 49%, which was similar to that in the discovery cohort. Moreover, no significant differences were observed in mutation types between

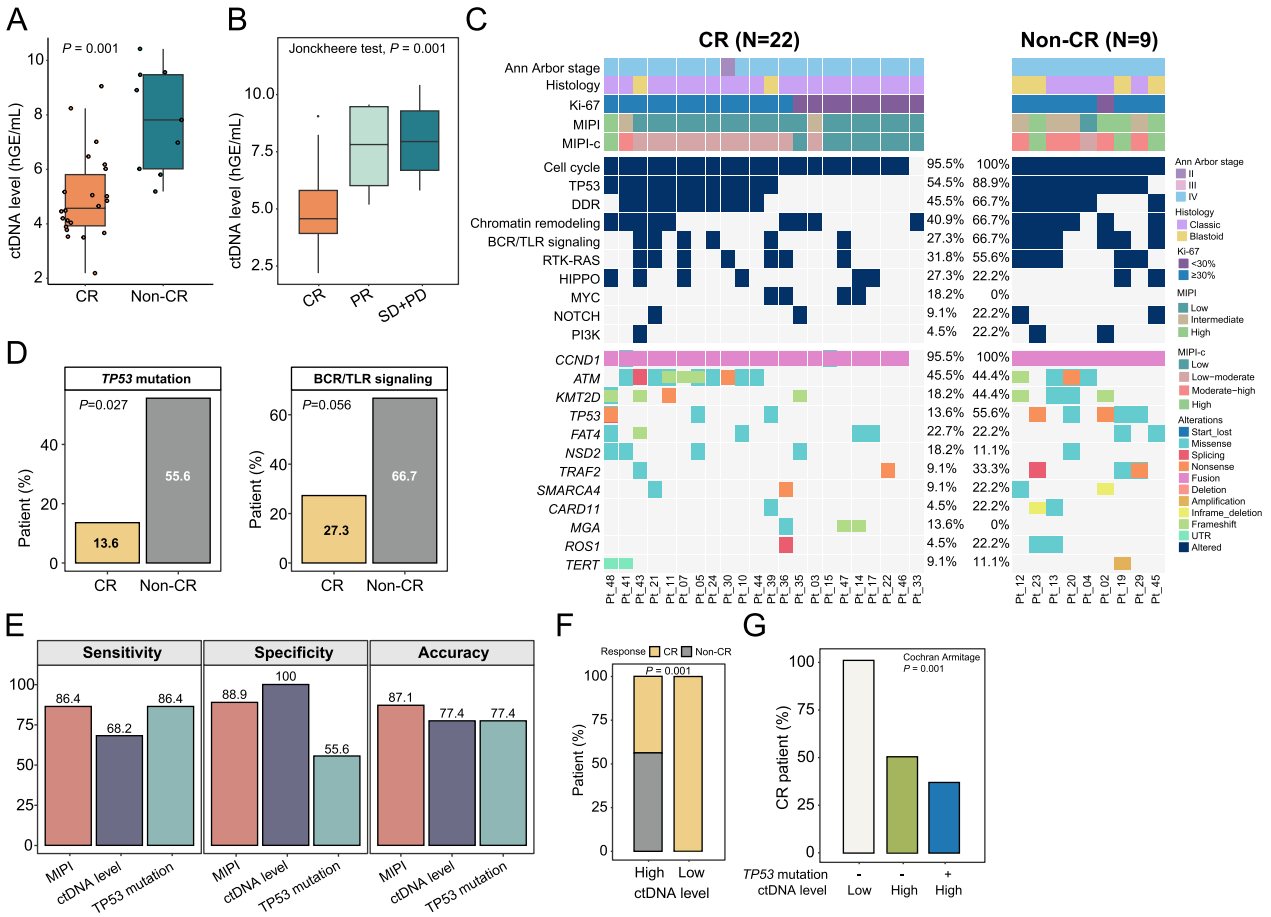


**Fig. 4** Predictive value of plasma ctDNA for treatment response. **A** Box plot showing the distribution of plasma ctDNA levels in patients with complete response (CR) and non-CR. **B** Higher ctDNA levels are associated with worse treatment response. (**C**) Mutation profiles of MCL patients grouped by treatment response, using plasma ctDNA for genotyping. (**D**) Bar plots depicting the proportion of CR and non-CR patients with *TP53* mutations or genetic alterations in the BCR/TLR signaling. (**E**) Comparison of ctDNA levels (using the median as the cutoff) and plasma-based *TP53* mutations in predicting treatment response, relative to the MCL International Prognostic Index (MIPI). (**F**) The proportion of CR and non-CR patients stratified by ctDNA levels, using the median ctDNA level as the cutoff. (**G**) The proportion of CR patients in subgroups stratified by both ctDNA level and the presence of *TP53* mutations

the cohorts (Supplementary Table S4). Therefore, we hypothesized that these discrepant findings may be due to differences in patient demographics and clinical characteristics. Additionally, due to differences in gene panel coverage (475 genes vs. 380 genes [33]), *TRAF2* and *TERT* mutations were absent in the external dataset. Further validation in larger cohorts with diverse populations is necessary to confirm these findings.

To explore the biological implications of mutations associated with disease progression and survival, we performed differential expression analysis using external microarray data from 43 MCL patients (Supplementary Fig. S5G-L). *TP53*-altered tumors were enriched in oxidative phosphorylation, thermogenesis, and neurodegeneration pathways, whereas *TP53*-unaltered tumors showed upregulation of pathways such as calcium signaling, neuroactive ligand-receptor interaction, natural killer mediated cytotoxicity (Supplementary Fig. S5 J). Meanwhile, *SMARCA4*-altered tumors exhibit enrichment in pathways associated with thermogenesis and lysine degradation, while *SMARCA4*-unaltered tumors displayed activation of immune-related pathways, including cytokine-cytokine receptor interactions, Toll-like receptor signaling, and viral protein interaction with cytokine and cytokine receptor, suggesting a more active immune microenvironment (Supplementary Fig. S5 K). KEGG analysis suggests that *ATM* alterations in MCL may promote a tumor environment with enhanced metabolic regulation and reduced inflammatory stress, which could contribute to the observed better prognosis (Supplementary Fig. S5L). However, further functional validation is needed to confirm these mechanistic links.

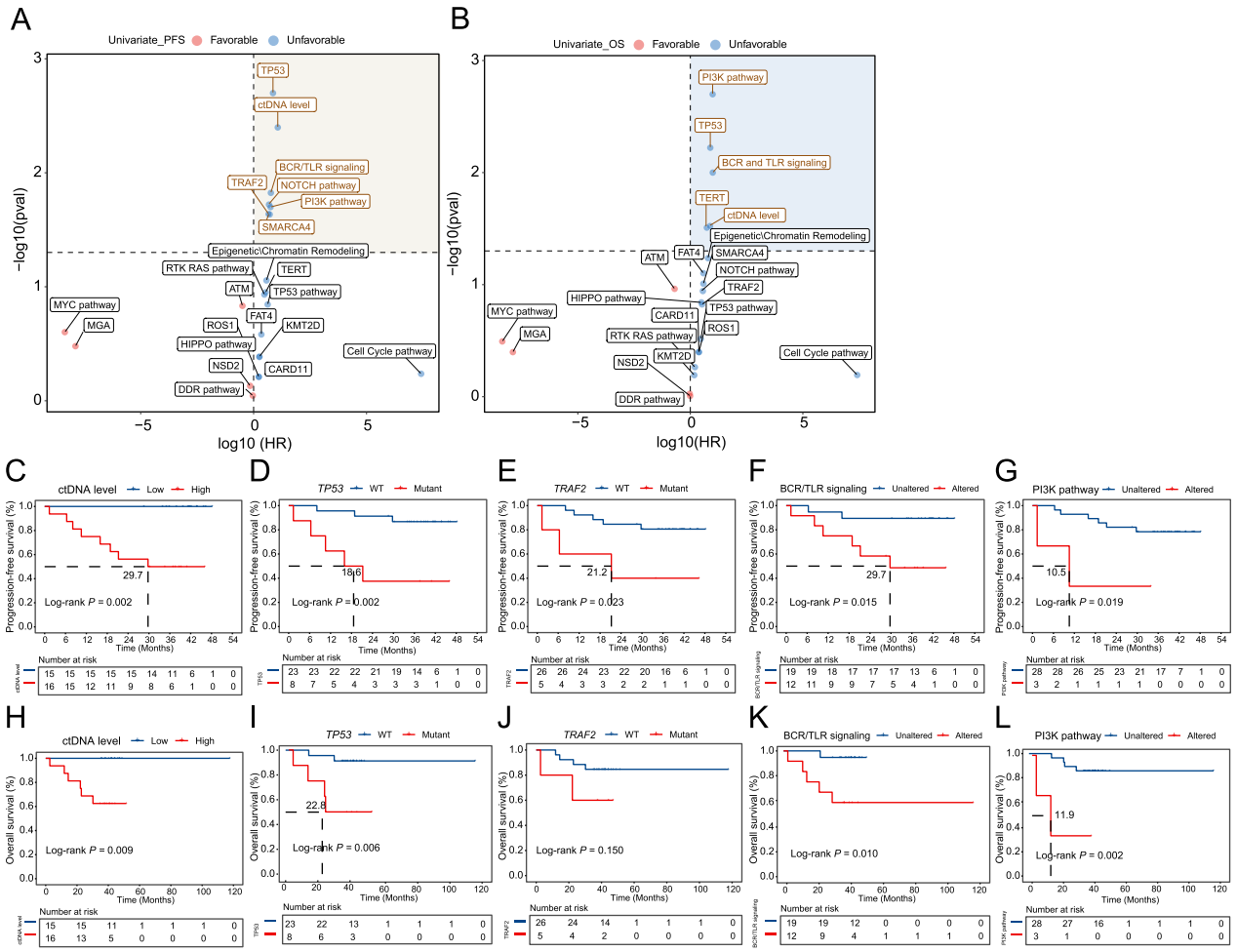


**Fig. 5** Prognostic association of plasma ctDNA in MCL patients. (**A, B**) Univariate Cox proportional hazard models for progression-free survival (A) or overall survival (B), based on baseline ctDNA levels and genomic features identified in plasma samples. (**C-G**) Kaplan–Meier survival curves showing the progression-free survival of patients stratified by ctDNA levels (using the median as cutoff) (C), *TP53* mutations (D), *TRAF2* mutations (E), and alterations in the BCR/TLR signaling pathway (F) and PI3K pathway (G). (**H–L**) Kaplan–Meier survival curves showing the overall survival of patients stratified by ctDNA levels (using the median as cutoff) (H), *TP53* mutations (I), *TRAF2* mutations (J), and alterations in the BCR/TLR signaling pathway (K) and PI3K pathway (L)

### Dynamic ctDNA changes predict molecular relapse before or at clinical progression

Finally, we examined the association between ctDNA dynamics and clinical outcomes in MCL. Among patients who achieved CR or partial response (PR), plasma samples collected during first-line therapy showed a significant decline in ctDNA levels compared to baseline ($P = 0.001$) (Supplementary Fig. S6). Here, we present two representative cases highlighting the potential of longitudinal ctDNA monitoring for disease surveillance and prognosis in MCL. Patient 48 (Pt_48) was diagnosed with stage IVb MCL, characterized by a high MIPI score and extensive metastases involving the terminal ileum, ascending colon, rectum, kidney, prostate, and bone marrow (Fig. 6A). Five serial plasma samples were analyzed using NGS, spanning from baseline through treatments and follow-up visits. Despite persistent ctDNA positivity, the variant allele frequency (VAF) of somatic mutations showed a marked decrease at the P2 and P3 time points, with no additional alterations compared to the baseline sample, aligning with a clinical assessment of complete remission (Fig. 6B, C). However, disease progression was detected through radiological imaging following maintenance therapy, which correlated with a positive ctDNA result at the P4 time point, showing increased VAFs of multiple mutations and the emergence of seven new mutations, indicative of molecular relapse and disease progression (Fig. 6C). After anti-CD19 CAR-T therapy, PET-CT scans revealed metabolically active tumor cells, while NGS profiling detected

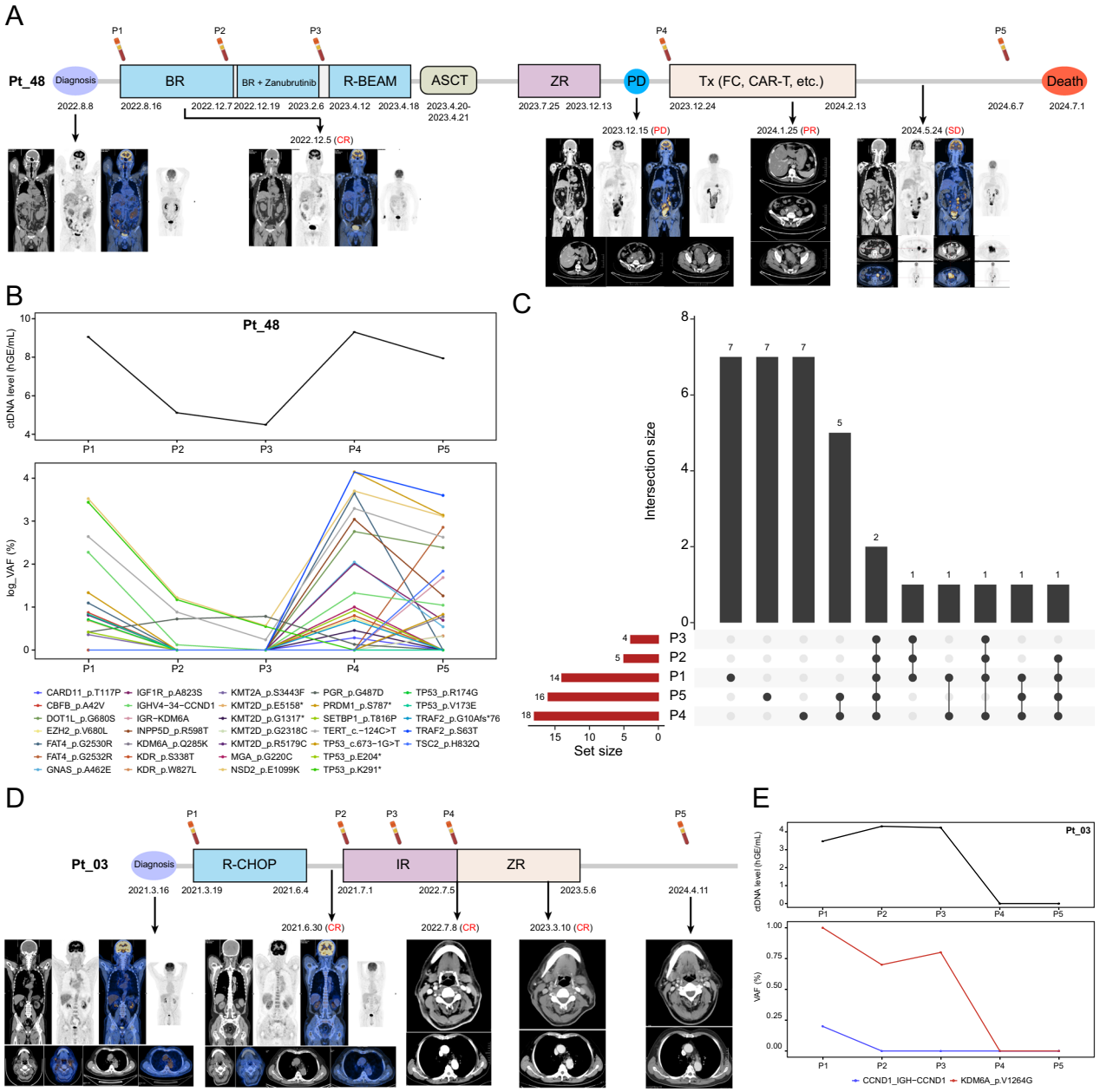


**Fig. 6** Longitudinal ctDNA monitoring for disease surveillance. (**A**) Timeline of treatment, plasma collection, and corresponding imaging results for patient 48 (Pt_48). After initial diagnosis, the patient was treated with rituximab and bendamustine (BR), with or without zanubrutinib, followed by the R-BEAM regimen (rituximab, carmustine, etoposide, cytarabine, melphalan), highlighted in blue. A complete response (CR) was achieved following BR treatment, as confirmed by PET-CT imaging. Following auto stem cell transplant (ASCT), the patient received maintenance therapy with the ZR regimen (zanubrutinib and rituximab), marked in purple. However, PET-CT revealed progressive disease (PD), and the patient was subsequently treated with fludarabine plus cyclophosphamide (FC) and anti-CD19 CAR-T therapy but ultimately passed away on July 1, 2024. (**B**) ctDNA levels and log-transformed variant allele frequency (VAF) of alterations in serial plasma samples for patient 48. (**C**) Upset plot showing the intersections of alterations across plasma ctDNA at five time points. (**D**) Timeline of treatment, plasma collection, and corresponding imaging results for patient 3 (Pt_03). The patient was initially treated with R-CHOP (rituximab, cyclophosphamide, doxorubicin, vincristine, and prednisone), achieving complete remission as confirmed by PET-CT scans. This was followed by subsequent maintenance treatments with the IR regimen (ibrutinib and rituximab) and the ZR regimen. Five longitudinal plasma samples were collected and analyzed using next-generation sequencing to monitor molecular changes over time. (**E**) ctDNA profiling showing the ctDNA levels and VAFs of detected alterations at various time points

additional mutations in plasma ctDNA at the P5 time point that were not previously identified, including FAT4_p.G2532R (VAF: 16.4%), TSC2_p.H832Q (VAF: 5.3%), KDM6 A-IGR fusion (VAF: 4.4%), PRDM1_p.S787* (VAF: 1.3%), KDM6 A_p.Q285 K (VAF: 1.2%), KDR_p.W827L (VAF: 0.4%), and KMT2D_p.G2318 C (VAF: 0.4%). The patient's disease progressed rapidly and passed away approximately 6.6 months after clinical progression. Another patient (Pt_03), diagnosed with stage IVA MCL and BM involvement, underwent first-line R-CHOP treatment and achieved a clinical complete response (Fig. 6D). Although the VAFs of mutations significantly decreased, the ctDNA level at the P2 time point was higher than at the baseline, prompting subsequent maintenance treatments with the IR and ZR regimens (Fig. 6E). Notably, the patient has remained ctDNA-negative and progression-free from the P4 time point to the most recent follow-up in April 2024. Collectively, these findings suggest that persistent ctDNA positivity may serve as an indicator of molecular relapse and progression, aligning with conventional radiological assessments, whereas undetectable ctDNA during surveillance may identify a subset of patients with favorable survival outcomes.

## Discussion

In this study, we assessed the clinical utility of plasma ctDNA for detecting tumor-specific genomic variants and its potential associations with treatment response and prognosis in MCL. Our findings highlight the high sensitivity of ctDNA in identifying recurrent mutations and clinically actionable genes in MCL. Genomic correlates of treatment response and prognosis detected in pretreatment plasma samples offer valuable insights for guiding early response-adapted therapies and developing tailored patient surveillance programs.

The clinical course and prognosis of patients with MCL are primarily determined by the specific pattern of molecular aberrations. However, tissue biopsies are invasive and subject to sampling bias, as they typically capture only a single region of the tumor and potentially missing subclone populations. On the other hand, radiographic imaging lacks the sensitivity and specificity needed for accurate diagnosis and disease monitoring. In stark contrast, plasma ctDNA, offers a more comprehensive and dynamic assessment of disease status, with a much lower detection threshold compared to imaging, allowing for a broader representation of the tumor's genetic landscape across various clinical settings. Nevertheless, this capability is underpinned by the strong concordance between gold-standard tissue biopsies and plasma ctDNA in detecting genomic variants, particularly recurrent mutations and clinically actionable genes. Our data showed that *CCND1*, *ATM*, *KMT2D*, *TP53*, *NSD2*, and *TRAF2* were among the most frequently mutated genes in MCL, regardless of sample types. Plasma ctDNA detected 66.3% of somatic genomic variants that were also present in paired tissue samples. This finding is consistent with Zhang et al., who reported a concordance rate of 69.8% in MCL patients with paired samples [34]. Notably, pretreatment plasma ctDNA exhibited exceptionally high sensitivity for identifying SVs, such as *CCND1* gene rearrangements, which serve as a molecular pathogenetic marker in MCL diagnosis. Furthermore, all *TP53* mutations and *SMARCB1* mutations identified in tissue biopsies were concurrently detected in plasma ctDNA, resulting in a sensitivity of 100%. It is worth noting that *TP53* mutations are an investigational prognostic biomarker associated with poor survival in MCL, as reported by both our data and others. In contrast, patients with hematologic tumors harboring oncogenic mutations in *SMARCB1* may benefit from treatment with tazemetostat [35].

We also compared genomic variants identified across paired tissue, plasma, and bone marrow aspirates. Using lymph node biopsy samples as the gold standard, our findings show that BM samples have limited capability for detecting CNVs, as all seven CNVs identified by tissue profiling were missed in BM. In contrast, 3 out of 7 (42.9%) CNVs were detected in plasma ctDNA, and all 18 SVs identified in tissue biopsies were also detected in plasma. Both sensitivity of detection and κ coefficients for individual genes, particularly recurrent mutations and those annotated by OncoKB, were lower in subgroup analysis comparing BM and tissue samples. Collectively, our preliminary results reinforce the clinical use of lymph node biopsies as the gold standard for definitive diagnosis, with plasma ctDNA serving as a complementary approach for variant detection. The accuracy of BM samples in detecting genomic variants, particularly diagnostic biomarkers, requires further investigation with larger sample sizes.

Early evaluation of therapeutic response provides a unique opportunity to tailor treatment strategies, while recognizing patients at higher risk of disease progression enables timely interventions to improve survival outcomes. Molecular analyses of pretreatment ctDNA are in demand to uncover biomarkers predictive of treatment response and inform prognosis. Consistent with previous research [36], our findings demonstrated that higher pretreatment ctDNA levels were associated with various established prognostic factors, underscoring its potential as a surrogate marker for disease burden. Notably, higher ctDNA levels and the presence of *TP53* mutations correlated with poor clinical responses and reduced survival. The prognostic significance of *TP53* mutations

was evident in baseline tissue samples and further validated using the external dataset. Transcriptional analysis revealed that *TP53*-altered tumors were enriched in pathways such as oxidative phosphorylation, thermogenesis, and neurodegeneration, which likely contribute to worse outcomes by promoting tumor aggressiveness and therapeutic resistance. *TRAF2* mutations emerged as an unfavorable biomarker associated with disease progression in both tissue and plasma profiling. Meanwhile, ctDNA-based mutations in *SMARCA4* and *TERT*, along with genetic alterations in the BCR/TLR, PI3K, and NOTCH pathways, were linked to inferior survival outcomes in MCL. These findings emphasize the clinical relevance of plasma profiling in identifying relevant mutations that may be missed in the original tissue biopsy. Indeed, prior research has linked ibrutinib resistance in MCL to somatic mutations in *TP53*, *TRAF2*, and *SMARCA4* [37]. SMARCA4 is a key component of the SWI/SNF chromatin remodeling complex and plays a pivotal role in the regulation of gene expression [38]. Mutations in *SMARCA4* are associated with resistance to resistance to ibrutinib and venetoclax combination therapy in MCL [39]. Our findings showed that *SMARCA4*-unaltered MCL patients had activated immune-related pathways, such as cytokine-cytokine receptor interactions and TLR signaling, suggesting a more active immune microenvironment and improved survival in patients without *SMARCA4* mutations. TERT is a critical enzyme for maintaining telomere length and genomic stability [40]. Mutations in *TERT* may contribute to cellular immortalization and tumorigenesis, ultimately leading to poorer clinical outcomes. Dysregulation of the BCR/TLR pathway and PI3K signaling may contribute to treatment resistance and poor survival of patients [41, 42]. Indeed, Bruton's tyrosine kinase inhibitors (BTKi) have demonstrated clinical efficacy in targeting BCR signaling. Ibrutinib, a covalent oral BTKi, achieved a 68% response rate in relapsed or refractory MCL and is currently approved for MCL treatment [43, 44]. Additionally, pirtobrutinib, the first non-covalent reversible BTKi, received accelerated FDA approval for relapsed or refractory MCL after two lines of systemic therapy. This was supported by promising results from the BRUIN Phase 1/2 trial (NCT03740529), which reported an overall response rate of 57.8% and a complete response rate of 20% [45]. Meanwhile, small-molecule inhibitors targeting PI3K, such as pan, isoform-specific and dual PI3K/mTOR inhibitors, have shown promise in hematologic malignancies by disrupting key survival and proliferation signals [46]. Building on these findings, future studies should explore the therapeutic potential of pathway-specific inhibitors, either alone or in combination with standard therapies, to improve patient outcomes.

Furthermore, our findings suggest that baseline *ATM* mutations were associated with a favorable prognosis in MCL patients. The *ATM* gene encodes a PI3K-related serine/threonine protein kinase essential for initiating DNA repair, and its dysregulation can lead to genomic instability [47, 48]. Indeed, 14 out of 22 tissue-based *ATM* mutations were oncogenic or "likely" oncogenic loss-of-function variants, resulting in ATM deficiency and synthetic lethality when exposed to DNA-damaging agents. We hypothesize that *ATM*-deficient tumors may exhibit increased genomic instability and heightened immunogenicity, potentially enhancing therapeutic responses and increasing susceptibility to chemotherapy. However, given the small sample size, the generalizability of these findings is limited, highlighting the need for validation in larger cohorts. Future studies with expanded patient populations and functional validation of *ATM* mutations are essential to confirm these mechanisms and further elucidate their clinical significance in MCL.

Last but not least, we highlighted the clinical utility of plasma ctDNA monitoring for disease surveillance in MCL. Our findings revealed that dynamic changes in ctDNA closely aligned with conventional radiological assessments of treatment response and prognosis. This was supported by two MCL cases: Pt_48, demonstrating persistent ctDNA positivity and increased VAFs of somatic mutations indicative of molecular disease progression, and Pt_03, who achieved ctDNA clearance following maintenance therapy, correlating with clinical progression-free clinical status and presumably a long-term survival benefit. Notably, ctDNA monitoring offers superior sensitivity and is free of radiological toxicity, allowing for earlier disease detection at lower thresholds than standard imaging techniques. However, it is important to acknowledge that the VAFs of individual somatic mutations do not always align with ctDNA levels, as demonstrated by Pt_03, where decreased VAFs were accompanied by an increased ctDNA level at the P2 and P3 time points compared to baseline. This discrepancy arises because the ctDNA level is determined by both the mean VAF and the cfDNA concentration. Despite the reduction in VAFs of the detected mutations, chemotherapy likely induced the release of cfDNA, offsetting the decreased VAFs and resulting in a higher ctDNA level. Therefore, it is recommended to monitor both ctDNA level and VAFs of individual mutations, in addition to conventional imaging approaches. Integrating molecular findings with a consideration of treatment-induced effects can provide a more comprehensive assessment, enabling more informed clinical diagnoses and treatment decisions.

We acknowledge the following limitations of the study, which necessitate further investigations. First, the small

sample size and single-center design presents significant challenges in data analysis, potentially affecting the robustness of statistical analyses and limiting the generalizability of our findings, particularly in subgroup comparisons. As the study mainly focused on conventional MCL and did not include other subtypes, such as leukemia-associated non-nodular MCL, this may affect the comprehensiveness of our results. Future studies with larger, multi-center cohorts and a broader inclusion of MCL subtypes are needed to validate these findings and enhance their clinical relevance. Second, given the known limitations of ctDNA in detecting CNVs, our results may underestimate the clinical significance of chromosomal-level changes in MCL detected in plasma. This limitation arises from several factors, including the inherent difficulty in detecting small CNVs (< 10 kb) due to signal-to-noise ratio issues and probe density limitations [49, 50], as well as technical challenges in reliably identifying low-frequency CNVs at low allele fractions [51, 52]. Future studies could address these challenges by developing more sensitive detection methods, optimizing sequencing depth and panel size, or integrating ctDNA analysis with complementary biomarkers, such as tissue-based or exosome-based sequencing, to enhance detection accuracy and reliability. Thirdly, the retrospective design of the study, which involves longitudinal plasma sample collection at varying time points across different treatment cycles, may not fully capture the dynamic changes in ctDNA during treatment and disease progression, potentially introducing variability in the analyses. Future prospective studies with standardized protocols for sample collection and analysis are necessary to overcome these limitations and enhance the robustness of the findings. Finally, while we have identified certain gene mutations associated with prognosis, an in-depth exploration of the molecular mechanisms underlying these mutations was not performed. Future studies focused on understanding the specific biological pathways involved will provide a more comprehensive understanding of the role these mutations play in MCL progression and treatment response.

## Conclusions

In conclusion, plasma ctDNA offers a noninvasive and effective method for capturing tissue-specific genetic aberrations, serving as a powerful complementary tool for variant detection in MCL. Plasma ctDNA provides critical insights into predicting treatment response and survival, enabling more effective and personalized treatment strategies in MCL patients.

### Abbreviations

| | |
|---|---|
| ASCT | Autologous stem cell transplantation |
| BCR | B cell antigen receptor |
| BM | Bone marrow |
| BTK | Bruton's tyrosine kinase |
| CAR-T | Chimeric antigen receptor therapy |
| cfDNA | Cell-free DNA |
| ctDNA | Circulating tumor DNA |
| CI | Confidence interval |
| CNV | Copy number variant |
| Indel | Insertion/deletion |
| CT | Computed tomography |
| CR | Complete response |
| hGE | Haploid genome equivalents |
| IGHV | Immunoglobulin heavy chain variable region |
| IQR | Interquartile range |
| KEGG | Kyoto encyclopedia of genes and genomes |
| LDH | Lactate dehydrogenase |
| HR | Hazard ratio |
| MCL | Mantle cell lymphoma |
| MIPI | MCL international prognostic index |
| NGS | Next-generation sequencing |
| OS | Overall survival |
| PD | Progressive disease |
| PET | Positron emission tomography |
| PFS | Progression-free survival |
| PR | Partial response |
| SNV | Single nucleotide variant |
| SOX-11 | Sex-determining regions-Y box transcription factor 11 |
| SD | Stable disease |
| SV | Structural variant |
| TERT | Telomerase reverse transcriptase |
| TCR | Toll-like receptor |
| VAF | Variant allele frequency |
| WHO | World health organization |

## Supplementary Information

The online version contains supplementary material available at https://doi.org/10.1186/s12935-025-03789-9.

Additional file 1.

Additional file 2.

### Acknowledgements

We would like to thank all the patients and family members who gave their consent to presenting the data in this study, as well as the investigators and research staff involved.

### Author contributions

Z. Ouyang: Conceptualization, formal analysis, investigation, methodology, writing–original draft. R.L. Zeng: Conceptualization, formal analysis, investigation, methodology, writing–original draft. S. Wang: Formal analysis, investigation, methodology, writing–original draft. X.Y. Wu: Formal analysis, investigation, methodology, writing–review and editing. Y.J. Li: Investigation, writing–review and editing. Y.Z. He: Investigation, writing–review and editing. C.Q. Wang: Investigation, funding acquisition, writing–review and editing. C. Xia: Investigation, writing–review and editing. Q.X. Ou: Investigation, writing–review and editing. H. Bao: Investigation, writing–review and editing. W. Yang: writing–review and editing. L. Xiao: Supervision, funding acquisition, resources, project administration, writing–review and editing. H. Zhou: Supervision, funding acquisition, resources, project administration, writing–review and editing.

### Funding

This study was supported by the National Natural Science Foundation of China (No. 82204414), the Precision Diagnosis and Treatment Center for Lymphoma in Hunan Province, Hunan Development and Reform Commission High-tech ([2021] No. 1073), the Hunan Provincial Natural Science Foundation of China (No. 2022 JJ30026, No. 2022 JJ30789), the Clinical Research Center for Lymphoma in Hunan Province, Hunan Provincial Clinical Medical Research Center for Lymphatic Tumors (No. 2021SK4015), and the National Key Clinical

Specialty Construction Project (No. 2023–223). The funder had no role in the study design, data collection, analysis, or decision to publish the manuscript.

**Availability of data and materials**
The datasets generated and/or analyzed during this current study are available from the corresponding author upon reasonable request. This study did not generate any unique code. All software and algorithms used in this study are freely or commercially available and are listed in the Methods section.

## Declarations

**Ethics approval and consent to participate**
The study was approved by the Ethics Committee of Hunan Cancer Hospital (No. 2024–152). Written informed consent was obtained from each patient before sample collection.

**Consent for publication**
Not applicable.

**Competing interests**
S. Wang, X.Y. Wu, Q.X. Ou, H. Bao, and W. Yang are employees of Nanjing Geneseeq Technology Inc. The remaining authors declare no competing interests.

**Author details**
[1]Department of Lymphoma and Hematology, The Affiliated Cancer Hospital of Xiangya School of Medicine, Central South University, Hunan Cancer Hospital, Changsha 410013, Hunan, China. [2]Geneseeq Research Institute, Nanjing Geneseeq Technology Inc., Nanjing 210032, Jiangsu, China. [3]Department of Histology and Embryology, School of Basic Medical Science, Central South University, Changsha 410013, Hunan, China.

Received: 28 February 2025 Accepted: 12 April 2025
Published online: 03 May 2025

**References**

1. Swerdlow SH, Campo E, Pileri SA, Harris NL, Stein H, Siebert R, et al. The 2016 revision of the World Health Organization classification of lymphoid neoplasms. Blood. 2016;127(20):2375–90.
2. Jain P, Wang ML. Mantle cell lymphoma in 2022—a comprehensive update on molecular pathogenesis, risk stratification, clinical approach, and current and novel treatments. Am J Hematol. 2022;97(5):638–56.
3. Silkenstedt E, Dreyling M. Mantle cell lymphoma-update on molecular biology, prognostication and treatment approaches. Hematol Oncol. 2023;41(Suppl 1):36–42.
4. Wen T, Wang J, Shi Y, Qian H, Liu P. Inhibitors targeting Bruton's tyrosine kinase in cancers: drug development advances. Leukemia. 2021;35(2):312–32.
5. Davis DD, Ohana Z, Pham HM. Pirtobrutinib: a novel non-covalent BTK inhibitor for the treatment of adults with relapsed/refractory mantle cell lymphoma. J Oncol Pharm Pract. 2024;30(1):182–8.
6. Wierda WG, Shah NN, Cheah CY, Lewis D, Hoffmann MS, Coombs CC, et al. Pirtobrutinib, a highly selective, non-covalent (reversible) BTK inhibitor in patients with B-cell malignancies: analysis of the Richter transformation subgroup from the multicentre, open-label, phase 1/2 BRUIN study. Lancet Haematol. 2024;11(9):e682–92.
7. Zhao S, Kanagal-Shamanna R, Navsaria L, Ok CY, Zhang S, Nomie K, et al. Efficacy of venetoclax in high risk relapsed mantle cell lymphoma (MCL)—outcomes and mutation profile from venetoclax resistant MCL patients. Am J Hematol. 2020;95(6):623–9.
8. Wang M, Munoz J, Goy A, Locke FL, Jacobson CA, Hill BT, et al. KTE-X19 CAR T-cell therapy in relapsed or refractory mantle-cell lymphoma. N Engl J Med. 2020;382(14):1331–42.
9. Hoster E, Dreyling M, Klapper W, Gisselbrecht C, van Hoof A, Kluin-Nelemans HC, et al. A new prognostic index (MIPI) for patients with advanced-stage mantle cell lymphoma. Blood. 2008;111(2):558–65.
10. Aukema SM, Hoster E, Rosenwald A, Canoni D, Delfau-Larue MH, Rymkiewicz G, et al. Expression of TP53 is associated with the outcome of MCL independent of MIPI and Ki-67 in trials of the European MCL network. Blood. 2018;131(4):417–20.
11. Bea S, Valdes-Mas R, Navarro A, Salaverria I, Martin-Garcia D, Jares P, et al. Landscape of somatic mutations and clonal evolution in mantle cell lymphoma. Proc Natl Acad Sci U S A. 2013;110(45):18250–5.
12. Eskelund CW, Dahl C, Hansen JW, Westman M, Kolstad A, Pedersen LB, et al. TP53 mutations identify younger mantle cell lymphoma patients who do not benefit from intensive chemoimmunotherapy. Blood. 2017;130(17):1903–10.
13. Yang P, Zhang W, Wang J, Liu Y, An R, Jing H. Genomic landscape and prognostic analysis of mantle cell lymphoma. Cancer Gene Ther. 2018;25(5–6):129–40.
14. Oki Y, Neelapu SS, Fanale M, Kwak LW, Fayad L, Rodriguez MA, et al. Detection of classical Hodgkin lymphoma specific sequence in peripheral blood using a next-generation sequencing approach. Br J Haematol. 2015;169(5):689–93.
15. Roschewski M, Dunleavy K, Pittaluga S, Moorhead M, Pepin F, Kong K, et al. Circulating tumour DNA and CT monitoring in patients with untreated diffuse large B-cell lymphoma: a correlative biomarker study. Lancet Oncol. 2015;16(5):541–9.
16. Scherer F, Kurtz DM, Newman AM, Stehr H, Craig AF, Esfahani MS, et al. Distinct biological subtypes and patterns of genome evolution in lymphoma revealed by circulating tumor DNA. Sci Transl Med. 2016;8(364):364ra155.
17. Rossi D, Diop F, Spaccarotella E, Monti S, Zanni M, Rasi S, et al. Diffuse large B-cell lymphoma genotyping on the liquid biopsy. Blood. 2017;129(14):1947–57.
18. Kurtz DM, Scherer F, Jin MC, Soo J, Craig AFM, Esfahani MS, et al. Circulating tumor DNA measurements as early outcome predictors in diffuse large B-cell lymphoma. J Clin Oncol. 2018;36(28):2845–53.
19. Spina V, Bruscaggin A, Cuccaro A, Martini M, Di Trani M, Forestieri G, et al. Circulating tumor DNA reveals genetics, clonal evolution, and residual disease in classical Hodgkin lymphoma. Blood. 2018;131(22):2413–25.
20. Desch AK, Hartung K, Botzen A, Brobeil A, Rummel M, Kurch L, et al. Genotyping circulating tumor DNA of pediatric Hodgkin lymphoma. Leukemia. 2020;34(1):151–66.
21. Camus V, Viennot M, Lequesne J, Viailly PJ, Bohers E, Bessi L, et al. Targeted genotyping of circulating tumor DNA for classical Hodgkin lymphoma monitoring: a prospective study. Haematologica. 2021;106(1):154–62.
22. Cheson BD, Fisher RI, Barrington SF, Cavalli F, Schwartz LH, Zucca E, et al. Recommendations for initial evaluation, staging, and response assessment of Hodgkin and non-Hodgkin lymphoma: the Lugano classification. J Clin Oncol. 2014;32(27):3059–68.
23. Bolger AM, Lohse M, Usadel B. Trimmomatic: a flexible trimmer for Illumina sequence data. Bioinformatics. 2014;30(15):2114–20.
24. Koboldt DC, Zhang Q, Larson DE, Shen D, McLellan MD, Lin L, et al. VarScan 2: somatic mutation and copy number alteration discovery in cancer by exome sequencing. Genome Res. 2012;22(3):568–76.
25. Liu SY, Bao H, Wang Q, Mao WM, Chen Y, Tong X, et al. Genomic signatures define three subtypes of EGFR-mutant stage II-III non-small-cell lung cancer with distinct adjuvant therapy outcomes. Nat Commun. 2021;12(1):6450.
26. Shen R, Seshan VE. FACETS: allele-specific copy number and clonal heterogeneity analysis tool for high-throughput DNA sequencing. Nucleic Acids Res. 2016;44(16): e131.
27. Shah Ronak. icallSV: A Framework to call Structural Variants from NGS based datasets. 2017; Available from: https://github.com/rhshah/iCallSV.
28. Shah Ronak. iAnnotateSV: Annotation of structural variants detected from NGS. 2021; Available from: https://github.com/rhshah/iAnnotateSV.
29. Huang X, He M, Peng H, Tong C, Liu Z, Zhang X, et al. Genomic profiling of advanced cervical cancer to predict response to programmed death-1 inhibitor combination therapy: a secondary analysis of the CLAP trial. J Immunother Cancer. 2021;9(5): e002223.
30. Yang Y, Wang J, Wang J, Zhao X, Zhang T, Yang Y, et al. Unrevealing the therapeutic benefits of radiotherapy and consolidation immunotherapy using ctDNA-defined tumor clonality in unresectable locally advanced non-small cell lung cancer. Cancer Lett. 2024;582: 216569.
31. Sanchez-Vega F, Mina M, Armenia J, Chatila WK, Luna A, La KC, et al. Oncogenic signaling pathways in the cancer genome atlas. Cell. 2018;173(2):321–37.

32. Chakravarty D, Gao J, Phillips SM, Kundra R, Zhang H, Wang J, et al. OncoKB: a precision oncology knowledge base. JCO Precis Oncol. 2017;2017:1–16.
33. Ma MCJ, Tadros S, Bouska A, Heavican T, Yang H, Deng Q, et al. Subtype-specific and co-occurring genetic alterations in B-cell non-Hodgkin lymphoma. Haematologica. 2022;107(3):690–701.
34. Zhang X, Yang L, Zhu M, Zhao X, Xiao Y, Pang J, et al. The clinical utility of plasma circulating tumor DNA in the diagnosis and disease surveillance in non-diffuse large B-cell non-Hodgkin lymphomas. Future Oncol. 2024;20:1–11.
35. Italiano A, Soria JC, Toulmonde M, Michot JM, Lucchesi C, Varga A, et al. Tazemetostat, an EZH2 inhibitor, in relapsed or refractory B-cell non-Hodgkin lymphoma and advanced solid tumours: a first-in-human, open-label, phase 1 study. Lancet Oncol. 2018;19(5):649–59.
36. Li M, Mi L, Wang C, Wang X, Zhu J, Qi F, et al. Clinical implications of circulating tumor DNA in predicting the outcome of diffuse large B cell lymphoma patients receiving first-line therapy. BMC Med. 2022;20(1):369.
37. Zhang L, Yao Y, Zhang S, Liu Y, Guo H, Ahmed M, et al. Metabolic reprogramming toward oxidative phosphorylation identifies a therapeutic target for mantle cell lymphoma. Sci Transl Med. 2019. https://doi.org/10.1126/scitranslmed.aau1167.
38. Mardinian K, Adashek JJ, Botta GP, Kato S, Kurzrock R. SMARCA4: implications of an altered chromatin-remodeling gene for cancer development and therapy. Mol Cancer Ther. 2021;20(12):2341–51.
39. Agarwal R, Chan YC, Tam CS, Hunter T, Vassiliadis D, Teh CE, et al. Dynamic molecular monitoring reveals that SWI-SNF mutations mediate resistance to ibrutinib plus venetoclax in mantle cell lymphoma. Nat Med. 2019;25(1):119–29.
40. Heidenreich B, Rachakonda PS, Hemminki K, Kumar R. TERT promoter mutations in cancer development. Curr Opin Genet Dev. 2014;24:30–7.
41. Fresno Vara JA, Casado E, de Castro J, Cejas P, Belda-Iniesta C, Gonzalez-Baron M. PI3K/Akt signalling pathway and cancer. Cancer Treat Rev. 2004;30(2):193–204.
42. Hua Z, Hou B. TLR signaling in B-cell development and activation. Cell Mol Immunol. 2013;10(2):103–6.
43. Wang ML, Rule S, Martin P, Goy A, Auer R, Kahl BS, et al. Targeting BTK with ibrutinib in relapsed or refractory mantle-cell lymphoma. N Engl J Med. 2013;369(6):507–16.
44. de Claro RA, McGinn KM, Verdun N, Lee SL, Chiu HJ, Saber H, et al. FDA approval: ibrutinib for patients with previously treated mantle cell lymphoma and previously treated chronic lymphocytic leukemia. Clin Cancer Res. 2015;21(16):3586–90.
45. Wang ML, Jurczak W, Zinzani PL, Eyre TA, Cheah CY, Ujjani CS, et al. Pirtobrutinib in covalent bruton tyrosine kinase inhibitor pretreated mantle-cell lymphoma. J Clin Oncol. 2023;41(24):3988–97.
46. Mishra R, Patel H, Alanazi S, Kilroy MK, Garrett JT. PI3K inhibitors in cancer: clinical implications and adverse effects. Int J Mol Sci. 2021;22(7):3464.
47. Choi M, Kipps T, Kurzrock R. ATM mutations in cancer: therapeutic implications. Mol Cancer Ther. 2016;15(8):1781–91.
48. Armstrong SA, Schultz CW, Azimi-Sadjadi A, Brody JR, Pishvaian MJ. ATM dysfunction in pancreatic adenocarcinoma and associated therapeutic implications. Mol Cancer Ther. 2019;18(11):1899–908.
49. Estivill X, Armengol L. Copy number variants and common disorders: filling the gaps and exploring complexity in genome-wide association studies. PLoS Genet. 2007;3(10):1787–99.
50. Mokhtar SS, Marshall CR, Phipps ME, Thiruvahindrapuram B, Lionel AC, Scherer SW, Peng HB. Novel population specific autosomal copy number variation and its functional analysis amongst Negritos from Peninsular Malaysia. PLoS ONE. 2014;9(6): e100371.
51. Ionita-Laza I, Laird NM, Raby BA, Weiss ST, Lange C. On the frequency of copy number variants. Bioinformatics. 2008;24(20):2350–5.
52. Le Tourneau C, Kamal M, Tsimberidou AM, Bedard P, Pierron G, Callens C, et al. Treatment algorithms based on tumor molecular profiling: the essence of precision medicine trials. J Natl Cancer Inst. 2016;108(4):djv362.


## Publisher's Note